Original Article

Study of quick diffusion of Fe on α-Zr by sectioning and LIBS techniques

Andrés Lucía [a,b,c,*], **Manuel Iribarren** [a,b], **Carolina Corvalán Moya** [a,c,d]

[a] *Comisión Nacional de Energía Atómica (CNEA), Av. Gral. Paz 1499 Buenos Aires, Argentina*
[b] *Instituto de Tecnología Jorge Sabato (UNSAM-IT Sabato), Buenos Aires, Argentina*
[c] *Universidad Nacional de Tres de Febrero (UNTREF), Buenos Aires, Argentina*
[d] *Consejo Nacional de Investigaciones Científicas y Técnicas (CONICET), Argentina*

ABSTRACT

Zirconium and its alloys are widely used in nuclear industry (nuclear fuel cladding tubes, structural materials, etc.) for its adequate properties under hostile conditions (corrosive environment, radiation damage, etc.) in the core of nuclear reactors.

In normal operating conditions, these materials present an important density of grain and interphase boundaries which act as quick paths for the movement of matter and can be in structural contact with Fe based alloys. The movement of fast diffusing elements (Fe, Co, Cr, Ni) in these short-circuit paths in Zr alloys [1] can produce technologically important inconveniences in nuclear reactors at normal service condition temperatures (low temperatures <600 K) like nucleation and growth of new phases [2] or complexions [3] and as a consequence, changes in their properties. Particularly, such diffusion process is fundamental for the development of Fe rich compounds in the alloy [4] as can affect its corrosion resistance [5] and mechanical properties.

In this work we present Fe diffusion measurements made on pure zirconium: volume, B and C kinetics in grain boundaries (GB) between 368 and 600 K.

The movement of fast diffusing elements (like Fe, Co, Cr, Ni) produces microstructural changes and technologically important inconveniences in nuclear reactors at normal service condition temperatures (low temperatures <600 K).

In this work, volume and grain boundaries (GB) diffusion of Fe in polycrystalline high purity Zr is measured using sectioning and LIBS technique between 368 and 600 K. Diffusion profiles, diffusion kinetics, segregation factor, Arrhenius plot, diffusion mechanisms and LIBS technique are discussed and, when possible, validated with existing data.

1. Introduction

The use of Zirconium alloys is widespread in the nuclear industry. In normal operating conditions, these materials present an important density of grain and interphase boundaries which act as quick paths for the movement of matter

* *Corresponding author.*
  E-mail: andreslucia@cnea.gov.ar (A. Lucía).

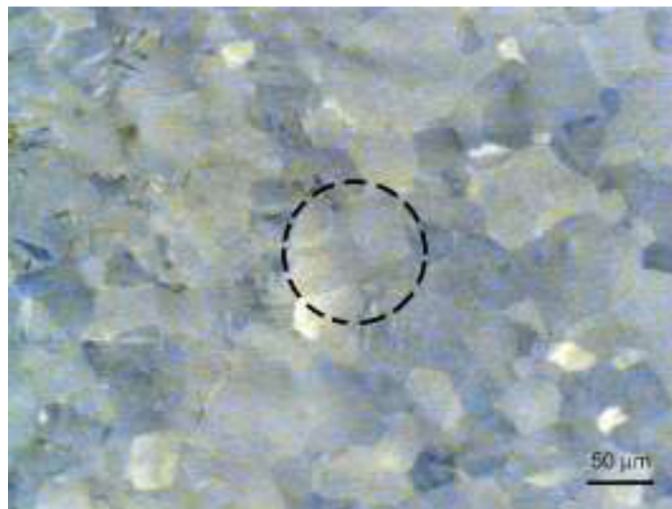| Table 1 – Pure Zr composition.							
Element	Al	C	Co	Cr	Cu	Fe	H	N
[ppmw]	5.00	9	<10	0.8	2.2	20	<1.0	<1.0
Element	**Nb**	**Ni**	**O**	**Si**	**Sn**	**Ti**	**W**	
[ppmw]	<0.1	9	11.0	5.0	2.00	<0.1	<0.1	

Fig. 1 – Pure Zr metallography showing small grain size for the samples. Dashed line shows approximate size of LIBS scanning area.

and can be in structural contact with Fe based alloys. The movement of fast diffusing elements (Fe, Co, Cr, Ni) in these short-circuit paths in Zr alloys [1] can produce technologically important inconveniences in nuclear reactors at normal service condition temperatures (low temperatures <600 K) like nucleation and growth of new phases [2] or complexions [3] and as a consequence, changes in their properties.

The use of Zirconium alloys is widespread in the nuclear industry.

Although most of its diffusion properties are well known, there are still some questions regarding matter mobility in grain boundaries, especially considering fast diffusing, low solubility elements, such as Fe. Particularly, such diffusion process is fundamental for the development of Fe rich compounds in the alloy [4] as can affect its corrosion resistance [5] and mechanical properties. The importance of this exceeds basic science; it is also a technologically relevant issue [6]. Because of this extremely low solubility in α-Zr [7], a very small quantity of Fe leads to contribute to the formation of a phase or complexion within the grain boundary, leading to a Fe rich zone more sensitive to corrosion [5]. Also, the strong segregation of this element can change the mechanical properties of the nuclear fuel cladding tube, which is the first security barrier to contain the products of the nuclear reaction within the reactor.

In the context of the lifetime of a nuclear power plant, a good characterization of nuclear fuel cladding tube is necessary. The knowledge of different processes at normal reactor temperatures (around 600 K) over a long time period (more than 20 years) is important. So, the localized diffusion of a bit of matter like the Fe diffusion inside the grain boundaries [8]

can generate phase transformation [9], segregation, etc. with consequences to the physical and chemical properties of the fuel cladding.

The aim of this work is to contribute to the knowledge of the behavior of nuclear fuel cladding tubes and propose new questions about the high diffusion of Fe at low temperatures.

1.1. Background

The first model to analyze grain boundary diffusion was proposed by Fisher [10] and modified by Gibbs with the Henry segregation isotherm to describe segregation effects [11]. Harrison [12] defined 3 different kinetics for the grain boundary diffusion: A, B and C. These kinetics depend on the relations between the parameters of the diffusion grain boundaries like grain size, diffusion paths on bulk and GB, etc. Type B kinetic involves both GB diffusion and volume diffusion. The volume diffusion field coming from one GB does not overlap the diffusion field coming from the other GB, so each of them can be treated as an isolated GB. In type C kinetics the most important process is GB diffusion. It is observed at low temperatures and/or extremely short annealing time. The diffusion only happens inside the GB. This kinetic regime is the only one that allows direct experimental measurement of the grain boundary diffusion coefficient. Combinations of measurements in B and C kinetics allow us to quantify the segregation. The first work about this was performed by Atkinson [13] for the diffusion of Ni in NiO. From 1992 up to now there is a systematic study of different systems to determine the segregation factor from diffusion measurements in B and C kinetics. Herzig, Mishin and Divinski, who worked with a

Table 2 – Temperature and times of diffusion anneals.

Sample	Kinetic	Temperature [K]	Annealing time [s]
1	B	600	58500
2	B	493	1209600
3–4	C	388	1800
5	C	378	5400
6–7	C	368	18000

radiotracer/sectioning technique, are the more representative authors on this subject: Fe in Cu [14], Ni in Cu [15], Bi in Cu [16], Co in Cu [17] and Co in Al [18], etc. In Argentina's Atomic Energy Commission, F. Dyment started a line of investigation in 1993 focused on grain boundaries and interface diffusion on Zr based alloys for nuclear applications [19]. In particular, Zr based systems had been studied with Co, Cr, Ni and Fe [1,19–21] as ultra-fast diffusing elements. At first it was only experimental data and now, for technological purposes, we are developing a kinetics Calphad database of Zr-based alloys [21,22].

In relation to the segregation phenomena, there are many existing analyses of this topic which generally classify segregation into three categories depending on its length range: macro, micro, and nanosegregation [23]. In this approach we are focused on nanosegregation. In this frame only a few layers are segregated in the grain boundaries. Furthermore, there is only an equilibrium segregation (like adsorption), where the relationship between bulk and grain boundary concentrations is the segregation factor. There are many diffusion works on the calculation of segregation factor from diffusion measurements in C and B kinetics [1,14–17].
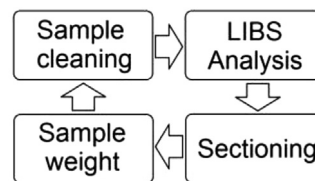
2. Materials and methods

Zr samples were obtained from a high purity (Table 1, Fig. 1), small grain size (15−20 μm), 6 mm rod provided by Material Research Corp. Seven 2.5 mm discs were cut and parallel polished up to 1000 grain size on one face. Iron deposit was performed with analytical grade $FeCl_3$ dissolved in distilled water, and then dried under Infrared light. We reserved two samples for type B kinetics measurements, which were wrapped in Ta foil and sealed in quartz tubes with a slight high purity Ar overpressure. For the remaining 5 lower temperature samples, one was wrapped in Ta foil, and the other four were packed in two ̈sandwich ̈type arrays using small Al presses specially crafted for this case. A Ta foil was used between the samples and the press to avoid Zr-Al contact and to capture any remaining O in the tube. They were then sealed in Pyrex tubes with a slight high purity Ar overpressure.

Thermal treatments times were calculated according to each kinetic condition [12], as shown in Table 2.

Diffusion anneals for samples 1 and 2 were conducted in conventional tubular furnaces with an accuracy of about ±1 K. Due to the short anneal times for samples 3–7, they were annealed in an ethylene glycol bath for a better thermal stability and heat transfer. This method allowed a greater accuracy of about ±0.2 K.

The concentration-depth profiles were obtained by a combined technique of sectioning using a precision grinding

Fig. 2 – Experimental process for the samples measurements.

machine and LIBS spectrometer [24,25]. Ten points distributed throughout the surface of the sample were measured, and the intensity of the resulting spectral lines for Zr and Fe were evaluated resulting in the relative concentration profile for each sample. Fig. 2 shows the sequence of the concentration profiles determination, and Fig. 3 shows the LIBS spectra for Fe and Zr lines.

The following equations were used for the calculation of P_{gb}(GB apparent diffusion coefficient from B kinetic) and D_{gb}(grain boundary diffusion coefficient from C kinetic) [1] and parameter α [14]. Where "s" is the segregation factor, D_v the diffusion bulk coefficient, δ is the grain boundary width, t is the anneling time and C corresponds to the relative concentration of Fe in the sample.

$$P_{gb} = s.\delta.D_{gb} = 1.3 D_v^{0.5} t^{-0.5} \left(-\frac{\partial lnC}{\partial x^{6/5}} \right)^{-5/3} \tag{1}$$

$$D_{gb} = \frac{-1}{4 \left(\frac{\partial lnC}{\partial x^2} \right) t} \tag{2}$$

$$\alpha = \frac{s.\delta}{2\sqrt{Dv.t}} \tag{3}$$

Parameter α actually works like a validation of C kinetic. α > 1 indicates the operation of C kinetic [14]. This will be addressed in Section 4.

3. Results

An example of the Fe (259.836 nm) line decreasing in relation to the depth of the Fe penetration in the Zr matrix is shown in Fig. 3. The Zr matrix line (339.197 nm) remains constant since the amount of Fe present in the sample is extremely low, as a required condition for the infinite dilution analysis. In [25] it was demonstrated that LIBS technique is suitable for the analysis of Zr-based alloys. For diffusion experiments such as our case, only relative concentration values are necessary for the evaluation of the penetration profile (similar to the radiotracer technique), avoiding the need for absolute concentration measurements.

The effective diffusion coefficient near to D_v value can be obtained from the first points of the B-kinetic profile in a ln(C)vs. x^2 plot, as shown in Fig. 4, using a variation of Eq. 2. This D_v value was used as a confirmation at low temperature of the values proposed by Herzig and used for the calculation of thermal anneals (Table 2) and P_{gb} (see Fig. 5) on this work.

The C-kinetic profile for 378 K is shown in Fig. 6. No segregation is involved in this profile as required by the C-kinetic
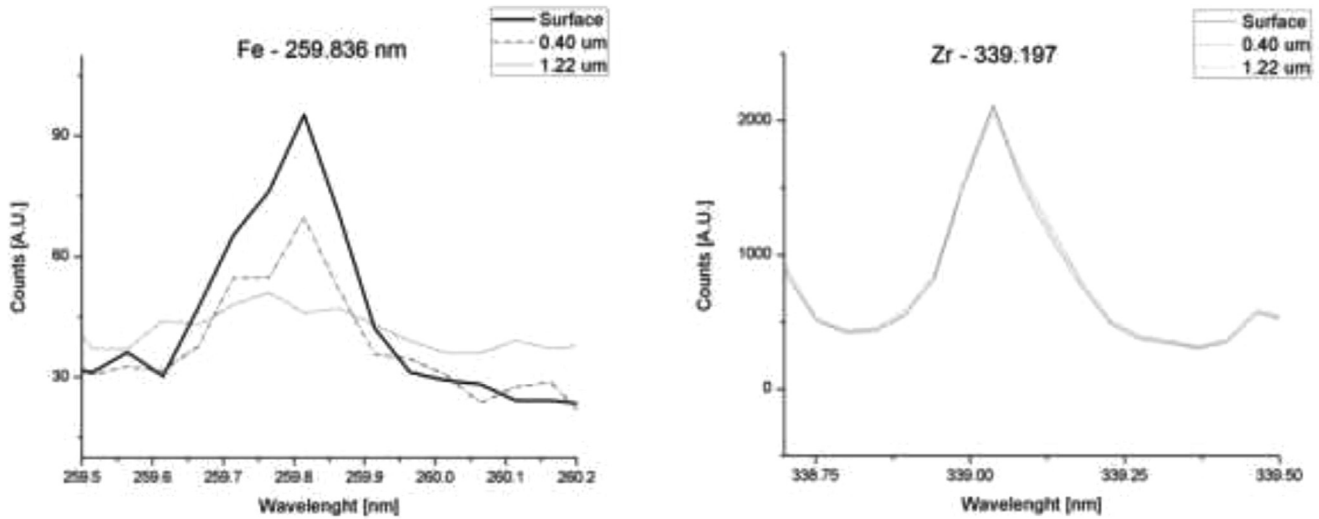
Fig. 3 – LIBS spectra for Fe (259.836 nm) and Zr (339.197) for different sample depths. Diffused Fe lines decrement intensity while Zr matrix remains constant.
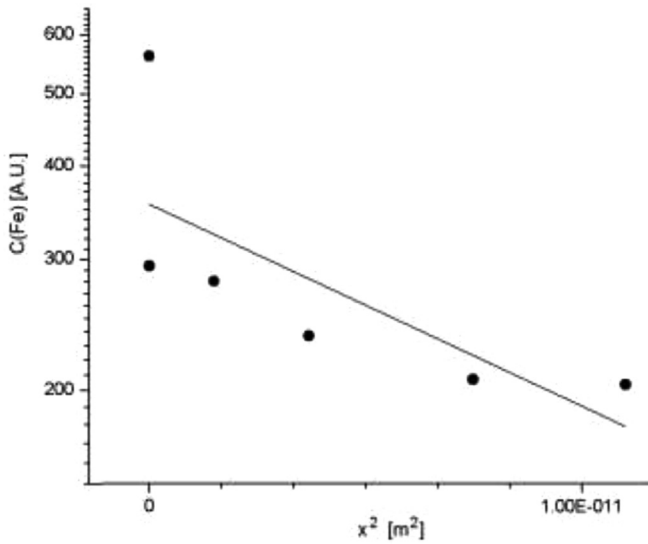

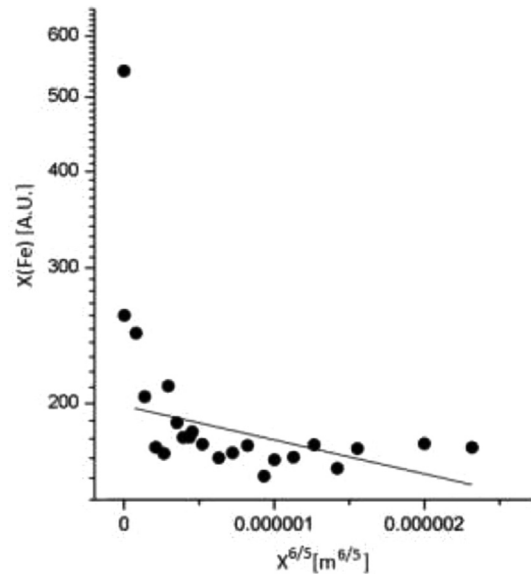**Fig. 4 – Diffusion profile for sample 1 (B kinetic) for D_v calculation. Shown as ln C(Fe) vs. x^2.**

Fig. 5 – Diffusion profile for sample 1 (B kinetic).Shown as ln C(Fe) vs.$x^{6/5}$.

limitations. Matter movement is exclusively inside the grain boundaries.

The arrhenius plot for the experimental B and C-kinetic diffusion values is shown next. D_{gb} values are multiplied by the grain boundary width (δ) in order to be compared to P_{gb}.

Calculated P_{gb}, D_{gb} and α (using Eq.1, Eq.2 and Eq. 3) from experimental data are shown in Table 3. The D_v values used for the calculations of P_{gb} were validated at low temperature from measurement of D_v, which is in good agreement with [1].
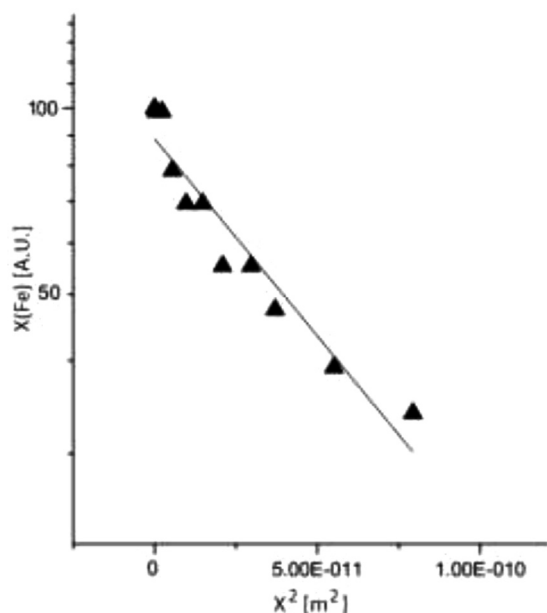
4. Discussion

4.1. Validation of LIBS technique

The first topic to be addressed is the validation for the experimental technique. LIBS has proven to be an adequate tool for

both the nuclear industry [26] and for Zr-based alloys analysis [25]. As shown by Ararat et al. [24], the sectioning and LIBS method is suitable for bulk diffusion. In our particular case, due to the extremely low quantities of material that move through the grain boundaries, several extra issues should be taken in consideration for the GB diffusion analysis. First, the detection level of the LIBS equipment has proven to be within reasonable limits for this experiment (traces below 1 ppm [27,28]). Although Fe was present in very low quantities, discrete Fe lines were clearly observed and identified (Fig. 3). Such lines were then used to calculate the concentration gradient and the P_{gb} and D_{gb} coefficients. Second, the percentage of the sample analyzed, in opposition with the traditional radio-tracer method, takes into account only a small portion of the material into consideration (about 5%) due to the laser spot

Table 3 – D_v (calculated with Herzig [1] data), P_{gb}, D_{gb} and α obtained from experimental data.

Sample	Temperature [K]	Time [s]	Kinetic	D_v[m^2/s]	D_{gb} [m^2/s]	P_{gb} [m^3/s]	α
1	600	58500	B	1.76E-16	–	2.23E-19	–
2	493	1209600	B	1.34E-19	–	1.76 E-21	–
3	388	1800	C	2.44E-24	2.19E-14	–	3.7
4	388	1800	C	2.44E-24	8.79E-15	–	3.7
5	378	5400	C	6.31E-25	6.21E-15	–	4.2
6	368	18000	C	1.51E-25	1.73E-16	–	4.8
7	368	18000	C	1.51E-25	2.41E-16	–	4.8

Fig. 6 – Diffusion profile for sample 5 (C kinetic).Shown as lnC(Fe) vs.x^2.

(of around 100 μm). Nevertheless, and thanks to the small grain size (about 15−20 μm), a single laser spot covered several GB. By averaging 10 shots in random places of the surface of the sample, the results turned out to be in good correlation with those presented by Herzig in [1], resulting in a positive validation of the method for this particular case in B kinetic. Nevertheless, this kind of analysis should be taken into consideration for the particular conditions of each systems (Fig. 7).

Regarding the P_{gb} and D_{gb} values calculated from the experimental data, we should divide the analysis in two parts. At higher temperatures (600 K and 493 K), B-kinetics experiments turned out in good correlation with those experimental data retrieved by Herzig [1], as shown in Fig. 8. We can see that, considering the differences in the experimental methods (radiotracer vs. LIBS), the data obtained in this work leads to validate the experimental sectioning-LIBS method used.

At the lower temperature (388 K, 378 K and 368 K), C-kinetic experiments show an abnormal behavior as compared with C-kinetic data in other systems [29,30], in which the C kinetic points seems to be several orders of magnitude lower than B-kinetic points at nearby temperature when comparing P_{gb} and $\delta.D_{gb}$. This matter will be addressed in section 4.2.The calculated Fe D_{gb} coefficients in this work are the first available data of C-kinetic measurements in α-Zr.

4.2. Segregation factor

The segregation is a local inhomogenity, particularly in our work we analyze this phenomenon at nanoscale, when only a few layers are involved around the GB. It can be an equilibrium or non-equilibrium segregation. The former only depends on both solute concentration and temperature; besides, only the final annealing conditions are relevant. The latter depends on microstructure and on thermal-mechanical history. If we consider that the GB represent a non-equilibrium crystal defect, all this thermodynamic equilibrium analysis can be questionable [31].

In this work we have considered the existence of an equilibrium linear segregation acting as a reversible process [32].Therefore it can be obtained from measurements in B and C diffusion kinetics, and the solute enrichment at any interface can be reproduced by re-establishing the identical physicochemical conditions. Finally, the local solute redistribution on GB is related to the minimization of the total Gibbs energy of the system. In any system, measurements in B and C kinetics (under similar conditions) lead to the direct calculation of the segregation factor by considering a direct comparison of the values obtained from the linear regression (and its extrapolation at lower temperatures) of B Kinetics measurements, P_{gb}, with the Type C kinetics scatter points, $\delta.D_{gb}$ (considering δ = 0.5 nm [14]). This can be seen in Fig. 9. From this comparison, a segregation factor near 1 can be achieved for Fe in α-Zr grain boundaries. As was previously remarked, this behavior is different to type B and C grain boundary diffusion experiments of Fe indifferent matrices [29,30].

4.3. D_v validation

The D_v values considered for the calculation of annealing times, P_{gb} and α are those extrapolated at each temperature from Herzig [1]. In order to reduce errors in the calculation, D_0 and Q data from both parallel and perpendicular to the c-axis data obtained by Nakajima [33] were also considered in the analysis, obtaining an arithmetical mean value as proposed by Vieregge [34], along with the self-diffusion of Zr (which usually stands around 10^8 lower). Although an extrapolation of D_v from higher temperatures may conduct an error when considering very low temperatures (no experimental data of D_v is available below 750 K [35]), the D_v calculated from the first points of the experimental 600 K profile (2.02E-16 m^2/s) showed a close match with both extrapolated values. The summary of this is shown in Fig. 10.
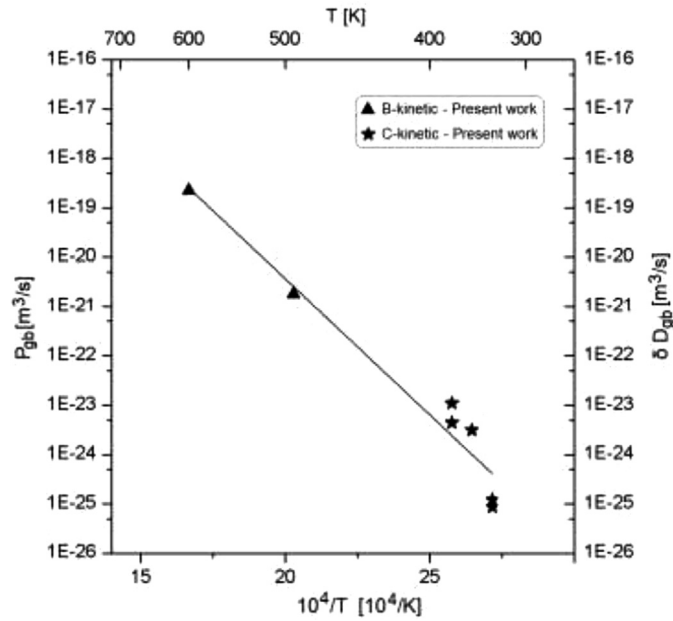
Fig. 7 – Arrhenius plot for experimental P_{gb} and $\delta.D_{gb}$ (B and C kinetic) data.
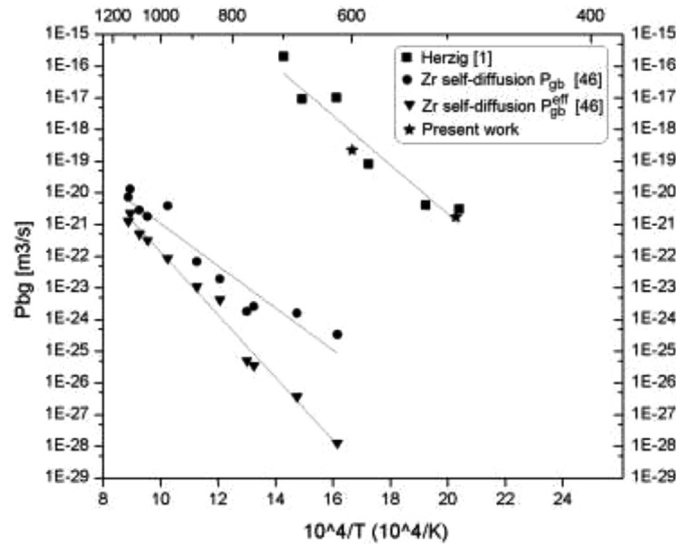

Fig. 8 – Arrhenius plot for different P_{gb} data of Fe in grain boundary of α-Zr and Zr grain boundary self-diffusion.

4.4. C kinetic

Experimental determination of grain boundary diffusion is prone to uncertainties [36,37]. The diffusion profiles in grain boundaries for different systems with a low solubility show normally significant deviations from the linear regression [29,30]. There are different aspects for that: 1) the surface segregation is significant, then the first points in the profile are not representative of the diffusion process on the grain boundaries, 2) the grain boundary diffusion considers a bit of matter in movement and it is located in a particular place (grain boundaries and surroundings), then this measure it is not an easy goal.

The correct determination of the diffusion kinetic is the key to a correct analysis of the profile and the subsequent calculation of diffusivity. As exposed by Harrison [12] and later developed by Ribbe [14], the value of the parameter α [Eq. 3] indicates the operating kinetic: $\alpha > 1$ corresponds to C-kinetic and $\alpha < 0.1$ corresponds to B-kinetic. The problem is that the segregation factor s is not known a priori and may depend on several factors such as non-linear solute segregation [38], low solubility of the diffuser, a dissociative mechanism for the bulk diffusion around GB [39] or the influence of lattice tensions from strong segregation [18,40]. For our case, the same strategy followed by Ribbe [14] was used: in case of C-kinetic, considering that the diffusion length in the crystallite bulk is negligible with respect to the GB width, $\delta/2 \sqrt{(Dv.t)} > 1$. Even a
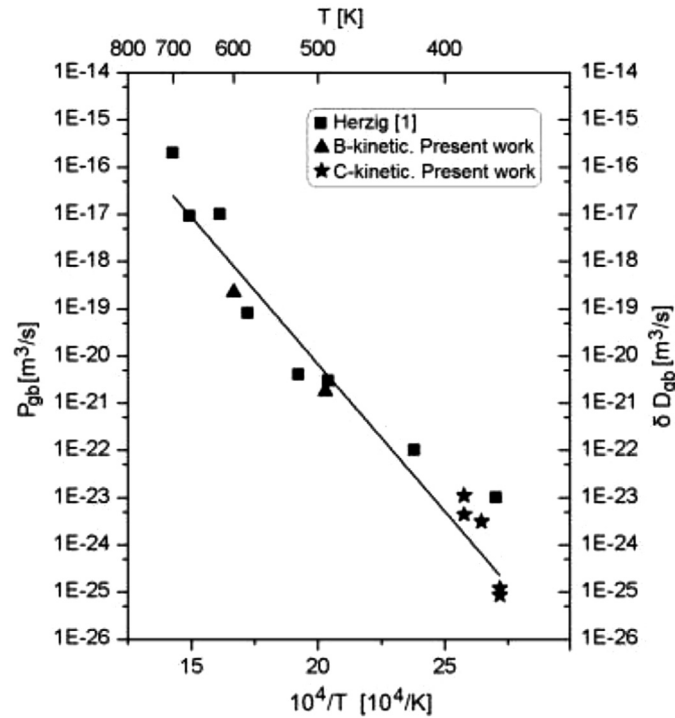
Fig. 9 – Arrhenius plot for Pgb and δ Dgb data.
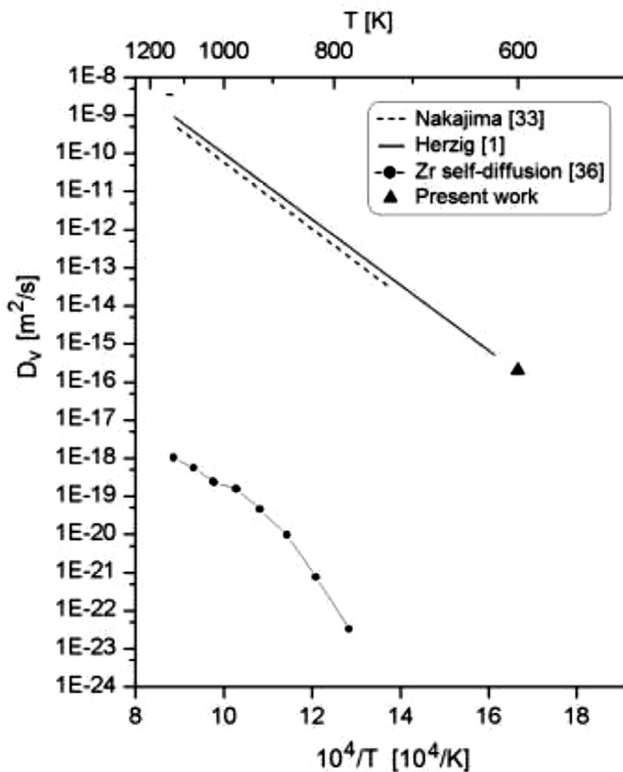

Fig. 10 – Arrhenius plot for different D_v data of Fe in α-Zr and Zr self-diffusion.

moderate segregation s > = 1 (due to the very low solubility of Fe in the alpha-Zr matrix), results in α > 1. In such conditions D_{gb}, can directly be calculated from the profile ln(C) vs. x^2. As

temperature increases, the segregation level has presumably to decrease. Since the bulk diffusivity increases, the value of α decreases significantly and the B-type regime conditions are promoted.

For our 388 K, 378 K and 368 K samples, α values were between 3.7 and 5, confirming pure C-kinetic diffusion mechanism and therefore considering matter movement exclusively in the GB. This allows the results analysis to be independent from the model of dissociative mechanism proposed by Mishin [39].

4.5. Grain boundary diffusion, volume diffusion and mechanism

Thinking the diffusion mechanism on grain boundaries like bulk diffusion mechanism result not enough to understand different phenomenological grain boundary kinetic process. We propose to consider the grain boundary as another phase, with its own thermodynamic and kinetic properties but with different atomic structure, in particular in our work with the same complexion formations [41,42].

The existence of complexions, as an equilibrium interfacial state [3,43], in addition to the extremely low solubility of Fe in the α phase of the Zr [7], may play an important role in the distortion of penetration profile at low temperatures measurements. As described by Pasianot [44], the formation of Fe dumbbells is energetically more convenient than the migration in the Zr matrix. This behavior may lead to the formation of a Fe-rich complexion which will take most of the Fe transported by the grain boundary, not allowing them into the Zr bulk. Further studies should be carried out to confirm or deny this theory, since the extremely low quantities of Fe

involved in the diffusion process in this cases does not allow easy acknowledgment of these small formations.

The existence of impurities in the GB may also affect the GB diffusion [45]. Segregation of low solubility - fast diffusers impurities (such as Co and Cr [21]) at low temperature may also contribute to the unusual behavior of this system, either by blocking tracer flux in triple junctions [46] or by combining with the tracer to form discrete complexions [3].

5.   Conclusions

B-kinetic values were obtained between 600 K and 493 K for the diffusion of Fe in Zr- grain boundaries. This values are in good correlation with those presented by Herzig in [1], resulting in a positive validation of the experimental method (LIBS/sectioning) for this case.

The grade of impurities in the base material seems to have very low incidence in the Fe diffusion in grain boundaries of Zr. Then the B kinetic diffusion values calculated in [1] and in this work are similar.

The combined technique of sectioning and LIBS proved to bea suitable technique to analyze diffusion process. Although certain considerations regarding the number of point taken by LIBS and the grain size of the sample should be taken into consideration.

Fe diffusion values in Zr grain boundaries (D_{gb} in C-kinetics) were obtained for 388 K, 368 K and 378 K. These are the first available data of C-kinetic measurements in this system.

Existing values of pre-exponential factor (D_0) and activation energy (Q) for volume diffusion (D_v) of Fe in Zr proposed by Herzig [1], previously available in the range of 1100 K to 750 K, were validated up to 600 K.

B-kinetic values obtained for 600 K and 493 K are in good correlation with those presented by Herzig in [1], resulting in a positive validation of the experimental method (LIBS/sectioning) for this particular case. Also, the grade of impurities in the base material used in [1] and in this work seems to have very low incidence in the P_{gb} data calculated from the experimental data.

The combined technique of sectioning and LIBS proved to be a suitable technique for this type of analysis, although certain considerations regarding the number of point taken by LIBS and the grain size of the sample should be taken into consideration.

Values of D_{gb} in C-kinetics were obtained for 388 K, 368 K and 378 K. These are the first available data of C-kinetic measurements in this particular system.

Author agreement

MSc. Andrés Lucia, Dr. Carolina Corvalan Moya and Dr. Manuel Iribarren, authors of the manuscript S̈tudy of quick diffusion of Fe on α-Zr by sectioning and LIBS techniques,̈ certify that all three of us have seen and approved the final version of the manuscript being submitted. We warrant that the article is the authors' original work, hasn't received prior publication and isn't under consideration for publication elsewhere.

Conflicts of interest

The authors declare no conflicts of interest.

Acknowledgements

REFERENCES

[1] Vierrege K, Willecke R, Herzig C. Grain Boundary diffusion of bulk interstitials in alpha-zirconium. Coll. de Phy 1990;51.

[2] Porter DA, Easterling KE. Phase transformations in metals and alloys. Chapman& Hall; 1992.

[3] Cantwell P, Tang M, Dillon SJ, Luo J, Rohrer GS, Harmer MP. Grain boundary complexions. ActaMaterialia 2014;62:1–48.

[4] Xiao W, Ma C. Study on the precipitates in Zry-4 by Mossbauer spectroscopy. J Nucl Mater 1998;255:67–71.

[5] Annanda K, Norda M, MacLarena I, Gassb M. The corrosion of $Zr(Fe, Cr)_2$ and Zr_2Fe secondary phase particles in Zircaloy-4 under 350 °C pressurized water conditions. Corros Sci 2017;128:213–23.

[6] Ahmad M, Akhter JI, Shaikh MA, Iqbal M, Ahmad W. Role of solute segregation on microstructure and mechanical properties of Zircaloy-4. J Mater Eng Perform 2003;12(2):179.

[7] Pérez RA, Weissmann M. Ab-initio approach to the effect of Fe on the diffusion in hcpZr. J Nucl Mater 2008;374:95–100.

[8] Bokstein B, Rodin A. Grain boundary diffusion and grain boundary segregation in metals and alloys. Diffus Found 2014;1:99–122.

[9] Raabe D, Herbig M, Sandlöbes S, Li Y, Tytko D, Kuzmina M, et al. Grain boundary segregation engineering in metallic alloys: a pathway to the design of interfaces. Curr Opin Solid State Mater Sci 2014;18:253–61.

[10] Fisher JC. Calculation of diffusion penetration curves for surface and grain-boundary diffusion. Appl. Phys 1951:74–84.

[11] Gibbs GB. Grain boundary impurity diffusion. Phys Status Solidi 1966;16:27.

[12] Harrison LG. Influence of dislocations on diffusion kinetics in solids with particular reference to the alkali halides. Trans. Faraday Soc 1961;57:1191–8.

[13] Atkinson A, Taylor RI. The diffusion of 63Ni along grain boundaries in nickel oxide. Philos Mag A 1981;43(4):979–98.

[14] Ribbe J, Esin VA, Divinski S. Grain boundary diffusion of 59Fe in high-purity copper. ActaMaterialia 2019;165:431–43.

[15] Divinski S, Ribbe J, Schmitz G, Herzig C. Grain boundary diffusion and segregation of Ni in Cu. ActaMaterialia 2007;55:3337–46.

[16] Divinski S, Lohmann M, Herzig C. Grain boundary diffusion and segregation of Bi in Cu: radiotracer measurements in B and C diffusion regimes. ActaMaterialia 2004;52:3973–82.

[17] Gaertner D, Wilde G, Divinski S. Grain boundary diffusion and segregation of 57Co in high-purity copper: radiotracer measurements in B- and C-type diffusion regimes. ActaMaterialia 2017;127:407–15.

[18] Divinski S, Kulitcki V, Kavakbasi BT, Gupta A, Buranova Y, Hickel T, et al. Grain boundary diffusion in severely deformed Al-based alloy. arxiv:1701.06694v1cond-mat.mtrl.sCi; 2017.

[19] Dyment F, Iribarren MJ, Vieregge K, Herzig C. Comparison between interphase and grain-boundary diffusion in zirconium-based materials. Philos Mag 1991;63(5):959.

[20] Pérez RA. Diffusion in very dilute Zr-Fe alloys. Defect Diffus Forum 2009;(283–286):128–32.

[21] Corvalán C, Lucia A, Iribarren M, Servant C. Costa e Silva A. Study and simulations of quick diffusion in Zr-based alloys. J Nucl Mater 2015;466:80–4.

[22] Dupin N, Ansara I, Servant C, Toffolon C, Lemaignan C, Brachet JC. A thermodynamic database for zirconium alloys. J Nucl Mater 1999;275:287–95.

[23] Lejcek P. Grain boundary segregation in metals. Springer series in materials science. Berlin, Heidelberg: Springer; 2010.

[24] Ararat-Ibarguen C, Pérez RA, Iribarren M. Measurements of diffusion coefficients in solids by means of LIBS combined with direct sectioning. Measurement 2014;55:571–80.

[25] Campbell KR, Judge EJ, Barefield JE, Colgan JP, Kilcrease DP, Czerwinski KR, et al. Laser-induced breakdown spectroscopy of light water reactor simulated used nuclear fuel: main oxide phase. SpectrochimicaActa Part B: Atomic Spectroscopy 2017;133:26–33.

[26] Barefield IIJE, Judge EJ, Campbell KR, Colgan JP, Kilcrease DP, Johns HM, et al. Analysis of geological materials containing uranium using laser-induced breakdown spectroscopy (LIBS). SpectrochimicaActa Part B: Atomic Spectroscopy 2016;120:1–8.

[27] Hahn D, Omenetto N. Laser-induced breakdown spectroscopy (LIBS), part II: review of instrumental and methodological approaches to material analysis and applications to different fields. ApplSpectrosc 2012;66(4):347–419.

[28] Martin M, Martin RC, Allman S, Brice D, Wymore A, Andre N. Quantification of rare earth elements using laser-induced breakdown spectroscopy. SpectrochimicaActa Part B 2015;114:65–73.

[29] Prokoshkina D, Esin VA, Divinski S. Experimental evidence for anomalous grain boundary diffusion of Fe in Cu and Cu-Fe alloys. ActaMaterialia 2017;133:240–6.

[30] Inoue A, Nitta H, Iijima Y. Grain boundary self-diffusion in high purity iron. ActaMaterialia 2007;55:5910–6.

[31] Bokstein B, Razumeiko BG, Rodin A. On equilibrium and stationary coefficients of grain boundary segregation. Defect Diffus Forum 2003;216–217:231–40.

[32] Polizzotti RS, Burton JJ. Surface segregation in alloys: dilute binary iron/zirconium solid solutions. J Vac Sci Technol 1977;14:347.

[33] Nakajima H, Hood GM, Schultz RJ. Diffusion of Fe in single-crystal α-Zr. Philosophical Magazine Part B 1988;58(3), 319-37.

[34] Vierrege K, Herzig C. Grain Boundary diffusion in a-Zr Part II: fast diffusing cobalt bulk interstitials. J Nucl Mater 1990;175:29–41.

[35] Mehrer H. Landolt-bornstein numerical data and functional relationships in science and technology, New series, group III: crystal and solid State physics. Diffusion in metals and alloys, Vol. 26. Berlin: Springer-Verlag; 1990.

[36] Horvath J, Dyment F, Mehrer H. Anomalous self-diffusion in a single crystal of α- zirconium. J Nucl Mater 1984;126:206.

[37] Bokstein B, Ostrovsky A, Bernardini J. Extraction of segregation term from the triple product of grain boundary diffusion: reconsideration of experimental data. Mater Sci Forum 1999;294–296:581–4.

[38] Bokstein B, Fradkov VE, Beke DL. Grain boundary segregation and grain boundary heterodiffusion. Philos Mag 1992;65(2):277–86.

[39] Mishin YM, Herzig C. Penetration profiles for fast grain-boundary diffusion by the dissociative mechanism. J Appl Phys 1993;73:8206.

[40] Larcht' FC, Cahn JI. The effect of self-stress on diffusion in solids. ActaMetallurgica 1982;30(10):1835–45.

[41] Tang M, Carter WC, Cannon RM. Grain boundary transitions in binary alloys. Phys Rev Lett 2006;97:075502.

[42] Esina V, Bokstein B, Rodin A. Concentration profiles for grain boundary diffusion in B-regime with regard to the formation of atomic complexes in grain boundary. Defect Diffus Forum 2011;309–310:29–38.

[43] Bokstein B, Rodin A, Smirnov A. Retardation effect of grain boundary segregation on grain boundary diffusion. Defect Diffus Forum 2006;249:167–72.

[44] Pasianot RC, Pérez RA. First-principles appraisal of solute ultra-fast diffusion in hcp Zr and Ti. J Nucl Mater 2013;434:158–61.

[45] Rodin A, Dolgopolov N, Pomadchik A. Concentration dependence of grain boundary diffusion. Defect Diffus Forum 2013;369(1662–9507):1–5.

[46] Vierrege K, Herzig C. Grain boundary diffusion in alpha-zirconium. Part I: self-diffusion. J Nucl Mater 1990;173:118–29.